Experimental and Molecular Pathology 111 (2019) 104321

Contents lists available at ScienceDirect

Experimental and Molecular Pathology

journal homepage: www.elsevier.com/locate/yexmp

Long non-coding RNA LINC00052 regulates miR-608/EGFR axis to promote progression of head and neck squamous cell carcinoma

Tianbin Ouyang[a], Ying Zhang[b,*], Shixiong Tang[a], Yaowen Wang[a]

[a] Department of Otolaryngology, The First Hospital of Ningbo, Ningbo City, Zhejiang Province 315010, China
[b] Department of Surgery, Guangzhou Eighth People's Hospital, Guangzhou Medical University, Guangzhou City, Guangdong Province 510060, China

ARTICLE INFO

Keywords:
LINC00052
HNSCC
miR-608
EGFR

ABSTRACT

An increasing number of studies have shown that long noncoding RNAs (lncRNAs) are dysregulated in cancers, and participate in cancer initiation and progression. LINC00052 is a newly identified lncRNA involved in tumorigenesis. However, the biological role and function of LINC00052 in head and neck squamous cell carcinomas (HNSCCs) is still unclear. In this study, we found that LINC00052 was upregulated in HNSCC tumors. High expression of LINC00052 was associated with poor prognosis. Gain and loss of function studies revealed that LINC00052 promoted HNSCC cell proliferation, migration and invasion. MiR-608 was predicted as an interacting microRNA of LINC00052 via bioinformatics analysis and was further validated through luciferase reporter assay and RNA-binding protein immunoprecipitation assay. Moreover, we demonstrated that LINC00052 sponged miR-608 to regulate the expression of epidermal growth factor receptor (EGFR), thereby promoting HNSCC progression in vitro and in vivo. Results from the current study provide evidences that LINC00052 acts as an oncogene in HNSCCs, and suggest LINC00052 is a potential therapeutic target for HNSCC treatment.

1. Introduction

Head and neck squamous cell carcinomas (HNSCCs), which are located in the oral cavity, oropharynx, hypopharynx, larynx or nasopharynx, account for over 90% of all head and neck cancers (Jou and Hess, 2017). HNSCCs are prevalent cancers with high mortality worldwide (Jou and Hess, 2017; Kolenda et al., 2017). It is believed that HNSCCs are strongly associated with tobacco smoking, alcohol consumption and human papillomaviruses (HPVs) infection (Leemans et al., 2018). Standard therapies for HNSCCs remain to be surgery, chemotherapy and radiotherapy (Jou and Hess, 2017; Wang et al., 2018). However, the 5-year survival rate has not been significantly improved (Wang et al., 2018). Therefore, better understanding the molecular biology of HNSCCs, especially the mechanisms of tumorigenesis, may provide new clues in treatment of HNSCCs.

Noncoding RNAs (ncRNAs) are RNA transcripts without protein-coding potential. It has been discovered that most of the transcriptome in mammalian cells is non-coding (Diamantopoulos et al., 2018). NcRNAs could be divided into two categories based on their length: ncRNAs below 200 nucleotides are referred as small noncoding RNAs (sncRNAs); and ncRNAs longer than 200 nucleotides are called long noncoding RNAs (lncRNAs) (Diamantopoulos et al., 2018). MicroRNAs are sncRNAs with 20–24 nucleotides and function by complementary binding the 3′ UTR of target mRNAs, which result in degradation of target mRNAs or translation suppression (Bartel, 2009; Fabian et al., 2010; Bartel, 2018). Increasing evidences show that lncRNAs and miRNAs are regulators in various cellular processes. Dysregulation of lncRNAs and miRNAs is associated with diseases, such as cardiovascular diseases, diseases of the central nervous system (Ni et al., 2018) and cancers (Liz and Esteller, 2016). Dysregulation of lncRNAs, such as HOTAIR, UCA1, LET, MEG3, MALAT1, H19 and NAG7, have been found in HNSCCs (Kolenda et al., 2017; Wang et al., 2018; Guglas et al., 2017).

EGFR is a transmembrane receptor for epidermal growth factor (EGF) and other ligands from the EGF family. Upon EGF binding, EGFR is activated and triggers downstream signalling pathways that lead to cell proliferation, migration and differentiation (Oda et al., 2005; Zhang et al., 2007). Overexpression of EGFR is linked with various cancers (Oda et al., 2005; Zhang et al., 2007), including HNSCCs (Bei et al., 2004; Ongkeko et al., 2005; Fung et al., 2015). Targeting EGFR by small molecule compounds and monoclonal antibodies is a strategy to control cancer progression (Zhang et al., 2007).

* Corresponding author at: Department of Surgery, Guangzhou Eighth People's Hospital, Guangzhou Medical University, No.8 Huaying Road, Baiyun District, Guangzhou City, Guangdong Province, China.
E-mail address: YingZhangsgh@163.com (Y. Zhang).

https://doi.org/10.1016/j.yexmp.2019.104321
Received 2 September 2019; Received in revised form 11 October 2019; Accepted 17 October 2019
Available online 19 October 2019
0014-4800/ © 2019 The Authors. Published by Elsevier Inc. This is an open access article under the CC BY-NC-ND license (http://creativecommons.org/licenses/BY-NC-ND/4.0/).

In this study, we found that lncRNA LINC00052 was upregulated in HNSCCs and associated with worse prognosis. We further demonstrated that LINC00052 acts as a decoy for miR-608 to alleviate the silencing effect of miR-608 on EGFR, thereby promoting progression of HNSCCs in vitro and in vivo. Findings from the current study indicate LINC00052 functions as an oncogene in HNSCCs, and suggest LINC00052 might be a potential therapeutic target for HNSCC treatment.

2. Materials and methods

2.1. Patients and tissue samples

A total of 65 HNSCC patients who received surgical resection in The First Hospital of Ningbo were enrolled in this study. The tumor tissues and adjacent nontumorous tissue samples were collected during surgical resection. This study was approved by the Ethical Committee of The First Hospital of Ningbo (Approval no.2018-R029), and all patients enrolled have given written informed consent.

2.2. Cell lines

CAL27 cells, FaDu cells and SCC9 cells were obtained from American Type Culture Collection (ATCC). SAS cells and HaCaT cells were obtained from FuHeng Biology (Shanghai, P.R. China). All cell lines were maintained in Dulbecco's modified Eagle's medium (DMEM) supplemented with 10% FBS (fetal bovine serum), and containing 1% penicillin-streptomycin (all from Gibco, Carlsbad, USA) in a humidified incubator containing 5% CO_2 at 37 °C.

2.3. Plasmids, oligonucleotides and transfection

cDNA of LINC00052 and coding sequence of EGFR was amplified and cloned into pcDNA3.1 vector. The shRNA constructs were generated using pLKO.1-puro vector. The target sequences for shRNA constructions were as follow: LINC00052 shRNA1: CAGAGGAAGTCAAAG ATATGG, LINC00052 shRNA2: ACCATGCAGTGATGTGAATAA, NC shRNA: ACGTGACACGTTCGGAGAATT. MiR-608 mimic, NC mimic, miR-608 inhibitor and NC inhibitor were purchased from Ribobio (Guangzhou, P.R. China).

Plasmids, miRNA mimics and miRNA inhibitors were transfected into FaDu cells and SAS cells using Lipofectamin 3000 (Invitrogen, Carlsbad, USA) according to manufacturer's protocol.

2.4. RNA isolation and RT-qPCR

Total RNA was isolated from tissues or cultured cells using TRIzol reagent (Sigma-Aldrich) following the manufacturer's instructions from the manual. 1 μg of total RNA was reverse transcribed into cDNAs using PrimeScript Reverse Transcriptase Reagent Kit (TaKaRa, Shiga, Japan). Then cDNAs were then subjected to quantitative PCR (qPCR) using Fast SYBR Green Master Mix (Applied Biosystems). Primer sequences for qPCR were as followed: LINC00052 Forwards: CCTGAAGTTT CTCCAT GAATTGTG, Reverse: GAGGGAGGGAGACTGAGATT; GAPDH Forwards: GGTCTCCTCTGACTTCAACA, Reverse: GTGAGGGTCTCTCT CTTCCT; EGFR Forwards: AACACCCTGGTCTGGAAGTACG, Reverse: TCGTTGGACAGCCTTCAAGACC.

For quantification of miRNA, small RNA was extracted using PrimeScript miRNA cDNA Synthesis Kit (TaKaRa, Shiga, Japan) following the manufacturer's instructions. RT-qPCR for miRNA was conducted using a TaqMan MicroRNA Assay Kit (Applied Biosystems, Foster City, USA) and qPCR primers for U6 snRNA (internal normalizer for miRNA) and mature miR-608 (Applied Biosystems) following the manufacturer's instructions.

2.5. Western blotting

Cultured cells and tissues were lysed in RIPA buffer (Beyotime, Shanghai, P.R. China).). Lysates were separated by 8–12% SDS-PAGE and then transferred to nitrocellulose membranes (Millipore, Bedford, USA). After blocking in 5% non-fat milk, the membranes were sequentially incubated with diluted primary antibodies and secondary antibodies. Signals were developed by adding Immobilon Western Chemiluminescent HRP Substrate (Millipore, Boston, USA) to the membranes and captured. Antibodies against E-cadherin, N-cadherin, EGFR, Ago2, Ki-67 and GAPDH, anti-mouse and anti-rabbit secondly antibodies were purchased from Cell Signalling Technology (Beverly, USA).

2.6. Cell proliferation assays

Cell proliferation ability was examined using a Cell Counting Kit-8 (CCK-8; Sigma-Aldrich) following the user's guide. For colony formation assay, the cells were collected 48 h post-transfection and re-plated into a 6-well plate. After 2 weeks, colonies were fixed using methanol and then stained using 0.1% crystal violet. The stained colonies were counted.

2.7. Cell migration assay and cell invasion assay

The assays were performed using transwell system (8-μm pore size, Corning). 48 h post-transfection, cells were harvested in serum-free medium and then seeded into the top side of a transwell filter uncoated (for migration assay) or coated (for invasion assay) with Matrigel (Sigma-Aldrich, USA). Medium supplemented with 10% FBS was added to the lower chamber. The cells were incubated at 37 °C for 24 h. Then the cells that migrated or invaded through the membrane were fixed with methanol and stained with 0.1% crystal violet. The stained cells were imaged and then counted in five random fields per well.

2.8. Isolation of cytoplasmic and nuclear RNA

Separation of nuclear and cytoplasmic fractions was performed using Protein And RNA Isolation System (PARIS) (Invitrogen) following the manufacturer's instructions. Briefly, cells were collected and incubated in ice-cold cell fractionation buffer. Samples were centrifuged to separate the nuclear (pellet) and cytoplasmic (supernatant) cell fractions. The pellet was further lysed in cell disruption buffer. The nucleus/cytoplasm lysates were mixed with 2× Lysis/Binding Solution and then 100% ethanol was added to the mixture. The RNA in the sample mixture was captured by a filter cartridge and eluted by adding elution buffer to the filter cartridge after washing.

2.9. Luciferase reporter assay

LINC00052 cDNA and the 3′ UTR of EGFR were cloned into pmirGLO Dual-Luciferase miRNA Target Expression Vector (Promega, Madison, USA). Mutations were generated by site-direct mutagenesis PCR reaction. All plasmid constructs were verified by DNA sequencing. Reporter plasmids were transfected into cells together with miRNA mimics. 48 h later, the luciferase activity was measured using the Dual-Glo Luciferase Assay System (Promega) following the guidance of user's manual.

2.10. RNA-binding protein immunoprecipitation assay (RIP)

RIP assay was conducted using the EZ Magna RIP kit (Millipore, Billerica, USA) following the manufacturer's protocol. Briefly, cells were lysed using RIP buffer and then incubated with magnetic beads conjugated with Ago2 antibody or control IgG at 4 °C for 6 h. After washing and incubation with Proteinase K, the immunoprecipitated

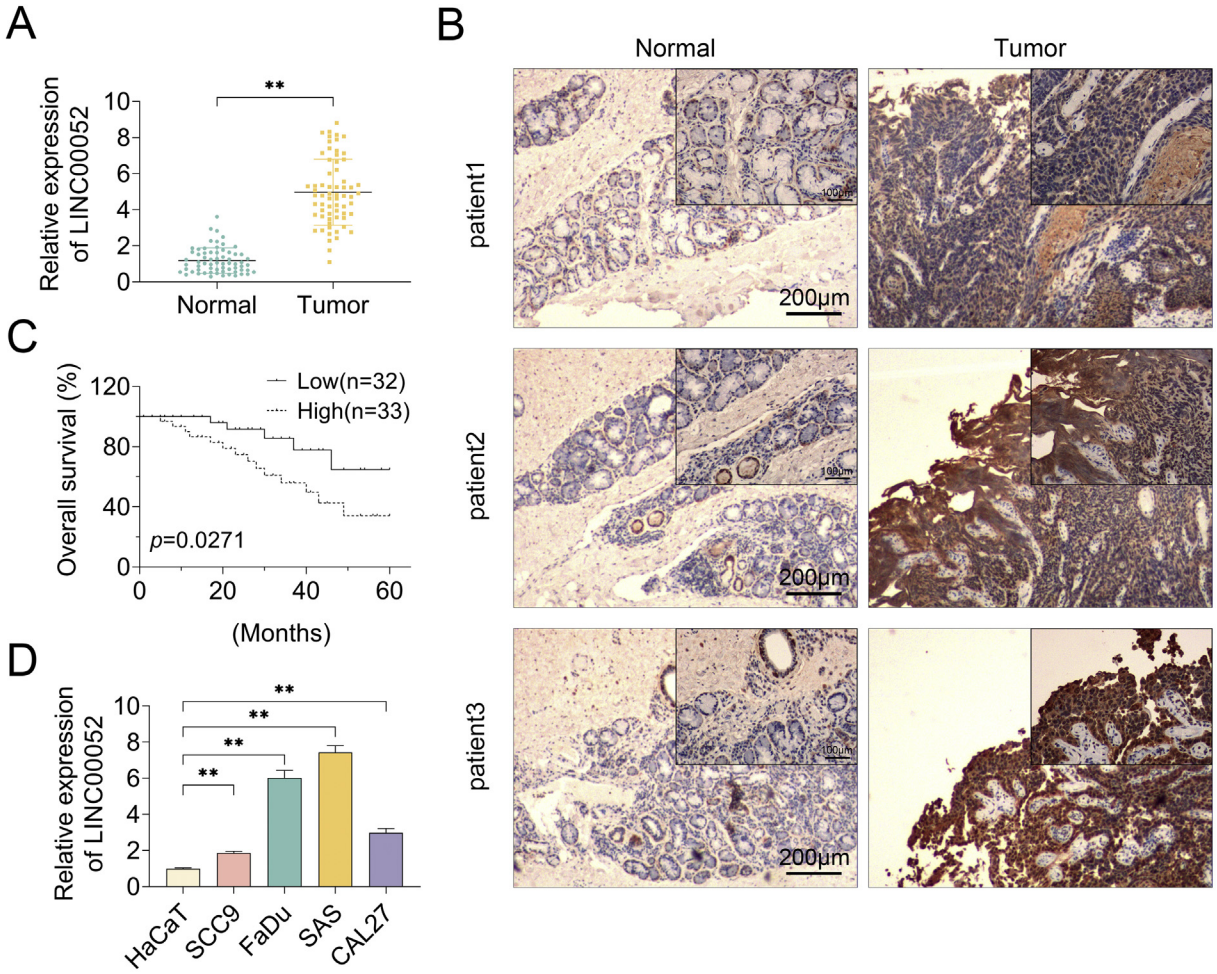

Fig. 1. LINC00052 was upregulated in HNSCCs.
(A) Tumor tissues and adjacent normal tissues were obtained from 65 HNSCC patients. RNA levels of LINC00052 in these samples were analysed via RT-qPCR assay. Significant differences were calculated using student's *t*-test. (B) ISH was performed to monitor the expression of LINC00052 in 3 pairs of patient tissues. (C) The patients were separated into two groups (low/high LINC00052 expression) with the median level of LINC00052 as a cut-off value. The overall survival curves of these two groups were plotted using the Kaplan-Meier method and estimated by log-rank test. (D) The expression levels of LINC00052 in the indicated cell lines were measured through RT-qPCR assay. Significant differences were calculated using one-way ANOVA. The data were presented as the mean ± SD of three independent experiments. $*p < .05$; $**p < .01$.

RNA was extracted and subjected to RT-qPCR.

2.11. In situ hybridization (ISH) and fluorescence in situ hybridization (FISH)

For ISH, tissues that were fixed in formalin and embedded in paraffin were cut into sections around 5 μm thick and mounted onto the slides. After drying, the slides were deparaffinized, rehydrated, digested with proteinase K for antigen retrieval, and dehydrated through ethanol (70%, 90%, and 100%). After air drying, the slides were incubated with Digoxigenin (DIG)-labeled RNA probe in hybridization buffer at 80 °C for 2 min. Hybridization was performed at 60 °C overnight. After stringency washes and drying, the slides were blocked and incubated with diluted anti-DIG antibody. The signal was developed with 3,3′-Diaminobenzidine (DAB), followed by hematoxylin staining.

For FISH, FaDu cells and SAS cells were fixed in 4% formaldehyde, washed and digested with proteinase K, and dehydrated through ethanol (70%, 90% and 100%). After air drying, the slides were incubated with Cy3-labeled RNA probe in hybridization buffer at 80 °C for 2 min. Hybridization was performed at 60 °C overnight. After stringency washes and drying, the slide was stained with DAPI for nucleus detection. DIG-labeled RNA probe and Cy3-labeled probe for LINC00052 were purchased from Ribobio (Guangzhou, P.R. China).

2.12. Immunohistochemistory (IHC)

Tissues fixed in formalin and embedded in paraffin were cut into sections around 5 μm thick and mounted onto the slides. After drying, the slides were deparaffinized, rehydrated, and then boiled for 30 min for antigen retrieval. After washing, the slides were blocked and immunostained for Ki-67, EGFR, and E-cadherin. The signal was developed with DAB, followed by hematoxylin staining.

2.13. Xenograft mouse model

Four-week-old female athymic BALB/c nude mice were obtained from Shanghai Laboratory Animal Center (Shanghai, P.R. China) and maintained in a pathogen-free environment. All procedures involving experimental animals were conducted in accordance with the Ethical Committee of Guangzhou Eighth People's Hospital, Guangzhou Medical University. To create an animal xenograft model of human HNSCC, FaDu cells were first transfected with sh-NC, sh-LINC00052, or sh-LINC00052 plus miR-608 inhibitor. 48 h post-transfection, 4×10^6 transfected FaDu cells suspended in 0.1 ml of sterile saline were subcutaneously inoculated into right flank of each mouse. When tumors were first palpable, the mice were intratumorally injected with Lipofectamine 3000-encapsulated sh-NC, sh-LINC00052, or sh-

LINC00052 plus miR-608 inhibitor every 3 days respectively. Tumors were measured for maximum (L) and minimum (W) length every three days, and tumor volumes were calculated as $L \times W^2/2$. On Day 21 post-inoculation, the mice were sacrificed and the tumors removed for weighting and further experiments.

2.14. Statistical analysis

Data were processed using software GraphPad Prism 5.0. Data were presented as the mean ± SD of at least three independent experiments. Significant differences were calculated using student's *t*-test or one-way ANOVA. Cox proportional hazards model multivariate analyses were used to evaluated the influence of LINC00052 expression and clinicopathological features on overall survival. *P* values < .05 were considered significant.

3. Results

3.1. LINC00052 was upregulated in HNSCCs and correlated with poor prognosis

To investigate the role of LINC00052 in HNSCCs, we first detected the expression level of LINC00052 in HNSCC tumor tissues. 65 paired HNSCC tumor tissues and adjacent nontumorous tissues were obtained from HNSCC patients. RNA was extracted from these samples and subjected to RT-qPCR assay. As shown in Fig. 1A, the expression of LIN00052 was significantly higher in HNSCC tumor tissues than in normal tissues. Results from ISH assay confirmed the upregulation of LINC00052 in HNSCC tumor tissues (Fig. 1B).

To explore the relationship between LINC00052 expression and clinicopathological features, we separated the tumor samples into a LINC00052 low expression group (below the median, $n = 32$) and a high expression group (equal to and above the median, $n = 33$). The overall survival curves of these two groups were plotted using the Kaplan-Meier method. We observed that patients with high LINC00052 expression had a lower overall survival rate (Fig. 1C). Moreover, high expression of LINC00052 was also significantly correlated with larger tumor sizes ($p = .017$), advanced clinical stages ($p = .008$), and lymph node metastasis ($p = .005$) in HNSCC patients (Table 1). High expressions of LINC00052 in tumors and the presence of lymph node metastasis were associated with a significantly higher risk of death (Table 2).

Table 1
Correlation between LINC00052 expression and clinicopathological parameters in HNSCC patients.

Parameters	No. of patients	LINC00052 expression		*P*-value*
		Low(< median)	High(≥median)	
Number	65	32	33	
Age				
< 59	31	17	14	0.388
≥59	34	15	19	
Gender				
Male	60	30	30	0.667
Female	5	2	3	
Smoking				
Yes	38	19	19	0.883
No	27	13	14	
Histological grade				
G1 + G2	25	12	13	0.875
G3	40	20	20	
T classification				
T1 + T2	37	23	14	0.017*
T3 + T4	28	9	19	
Clinical stage				
I + II	26	18	8	0.008*
III + IV	39	14	25	
Lymph node metastasis				
N0	43	27	16	0.005*
N+	22	5	17	

* $P < .05$ was considered statistically significant.

Table 2
Cox model analysis of overall survival.

Parameters	Relative risk (95% CI)	*P*-value
Univariate		
Age	0.692(0.277–1.727)	0.430
Gender	1.214(0.279–5.274)	0.796
Smoking	1.738(0.705–4.285)	0.230
Histological grade	0.991(0.398–2.468)	0.984
T classification	5.364(1.919–14.996)	0.001
Clinical stage	6.628(1.913–22.962)	0.003
Lymph node metastasis	17.584(5.059–61.122)	0.000
LINC00052 expression	2.983(1.074–8.284)	0.036
Multivariate		
Lymph node metastasis	21.936(2.554–188.422)	0.005

3.2. LINC00052 regulated HNSCC cell proliferation, migration and invasion

To assess the effects of LINC00052 on cellular processes, we first examined the expression of LINC00052 in HNSCC cell lines, including SCC9, FaDu, SAS, CAL27, and the human immortalized keratinocyte cell line, HaCaT. We found that LINC00052 mRNA expression levels were significantly higher in HNSCC cells compared with HaCaT cells (Fig. 1D). FaDu cells and SAS cells expressed relatively higher levels of LINC00052 among these HNSCC cells, and were chosen for further investigation.

A plasmid expressing LINC00052 (pcDNA3.1-LINC00052) was constructed and transfected into FaDu cells and SAS cells (Fig. 2A). CCK-8 assays revealed that overexpression of LINC00052 modestly promoted HNSCC cell proliferation (Fig. 2B). However, the difference was significant (Fig. 2B). This result was further confirmed by colony formation assays (Fig. 2C). Using transwell experiments, we observed that overexpression of LINC00052 increased the migration and invasion potential of FaDu cells and SAS cells (Fig. 2D–E). Analysis of the epithelial marker *E*-cadherin and the mesenchymal marker N-cadherin revealed that overexpression of LINC00052 reduced E-cadherin and increased N-cadherin (Fig. 2F), indicating the induction of epithelial-mesenchymal transition (EMT), which is critical for tumor invasion.

To deplete LINC00052 in HNSCC cells, plasmids expressing shRNAs targeting LINC00052 were generated. Both of the shRNAs depleted the expression of LINC00052 (Fig. 3A) and suppressed cell proliferation as shown by CCK-8 assays (Fig. 3B). sh-LINC00052#2 showed better effect on LINC00052 depletion and cell proliferation suppression (Fig. 3A&B), and was used in further experiments. Consistent with Fig. 3B, results from colony formation assays also showed that depletion of LINC00052 in HNSCC cells suppressed cell proliferation (Fig. 3C). Knockdown of LINC00052 by shRNA also impaired the ability of migration and invasion of HNSCC cells (Fig. 3D–E). Moreover, sh-LINC00052 cells expressed lower level of N-Cadherin and higher level of E-Cadherin (Fig. 3F), which was indicative of less EMT. Taken together, these data demonstrated that LINC00052 facilitated proliferation, migration and invasion of HNSCC cells.

3.3. LINC00052 interacted with and regulated miR-608 in HNSCC cells

Accumulating studies have demonstrated that lncRNAs may serve as competing endogenous RNAs (ceRNAs) to bind miRNAs in cytoplasm, thereby alleviating the silencing effect of miRNAs on their target mRNAs (Liz and Esteller, 2016). To test whether LINC00052 functions as a ceRNA, we first examined the distribution of LINC00052 in HNSCC cells. FaDu cells and SAS cells were fractionated into nuclear and

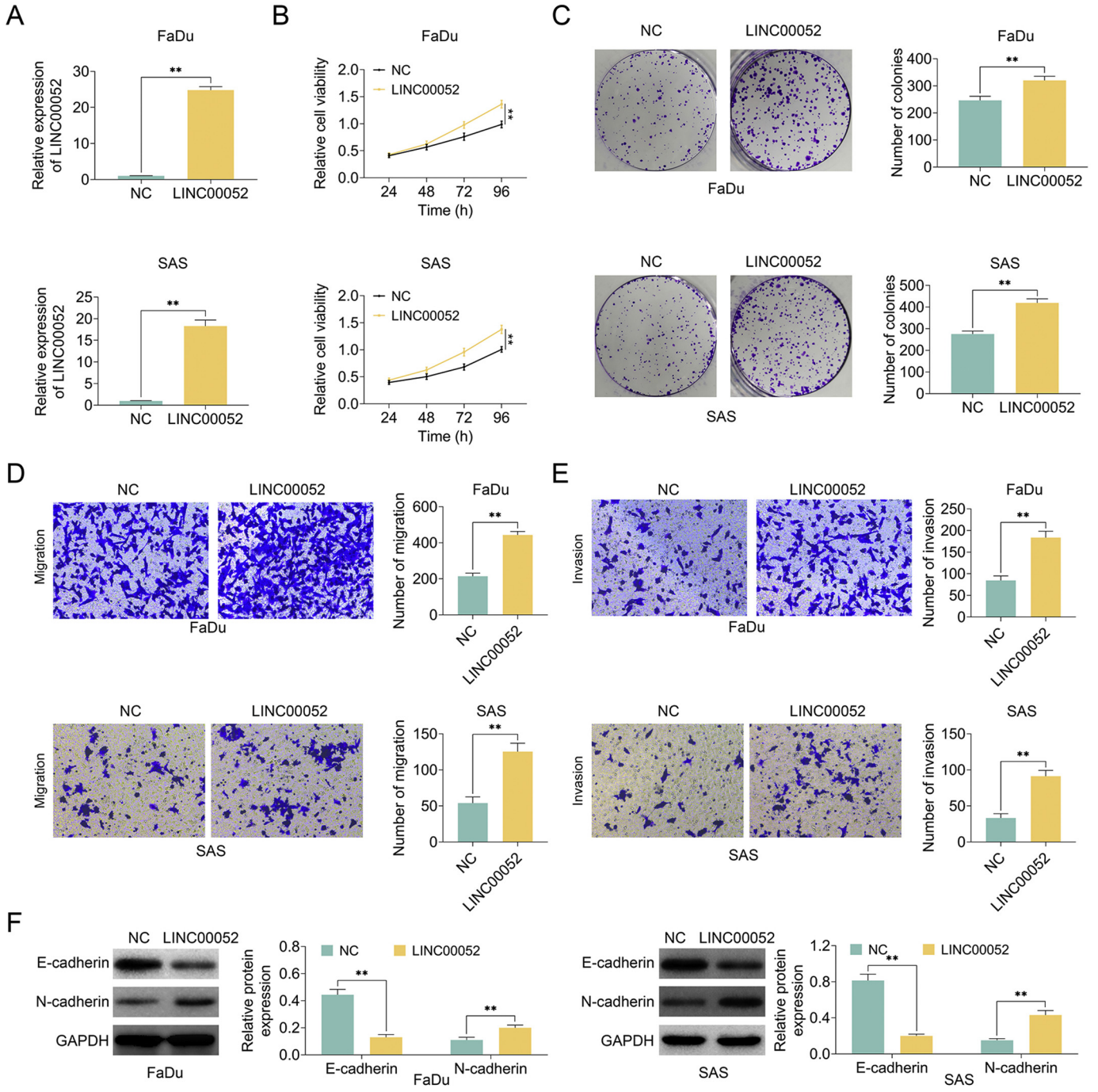

Fig. 2. Overexpression of LINC00052 promoted HNSCC cell proliferation, migration and invasion.
HNSCC cell line FaDu and SAS were transfected with pcDNA3.1 vector (negative control, NC) or pcDNA3.1-LINC00052 plasmid. The RNA levels of LINC00052 were analysed via RT-qPCR assay (A). Transfected cells were subjected to CCK-8 assay (B), colony formation assay (C), cell migration assay (D), cell invasion assay (E), and western blotting assay with the indicated antibodies (protein expression was normalized to GAPDH and shown as relative protein expression) (F). The data are presented as the mean ± SD of three independent experiments. Significant differences were calculated using student's *t*-test. $*p < .05$, $**p < .01$.

cytoplasmic components. Subsequent RT-qPCR assays revealed that LINC00052 was mainly distributed in cytoplasm (Fig. 4A), which was further confirmed by FISH assay (Fig. 4B). Next, we performed a mining to identify potential miRNAs that interact with LINC00052 using microRNA target prediction tool miRSearch 3.0 (https://www.exiqon.com/miRSearch) and found that miR-608 contains a complementary site with LINC00052 (Fig. 4C). To validate this predicted interaction, we constructed luciferase reporters containing either the wildtype or mutated LINC00052 (WT or MUT pmirGLO-LINC00052) (Fig. 4C). These reporters together with miR-608 mimic were transfected into FaDu cells and SAS cells. Results of dual luciferase assays showed that miR-608 mimic reduced the luciferase activity of wildtype pmirGLO-LINC00052, but not the mutated pmirGLO-LINC00052 (Fig. 4D). MicroRNAs and the RNA targets are present in the same RNA-induced silencing complex (RISC), which also contains Ago2. To further confirm that miR-608 and LINC00052 are in the same RISC, RNA-binding protein immunoprecipitation (RIP) assays were performed on FaDu and SAS cell lysates using Ago2 antibody. As shown in Fig. 4E, the level of LINC00052 and miR-608 was both higher in Ago2-immunoprecipitation than that in IgG-immunoprecipitation.

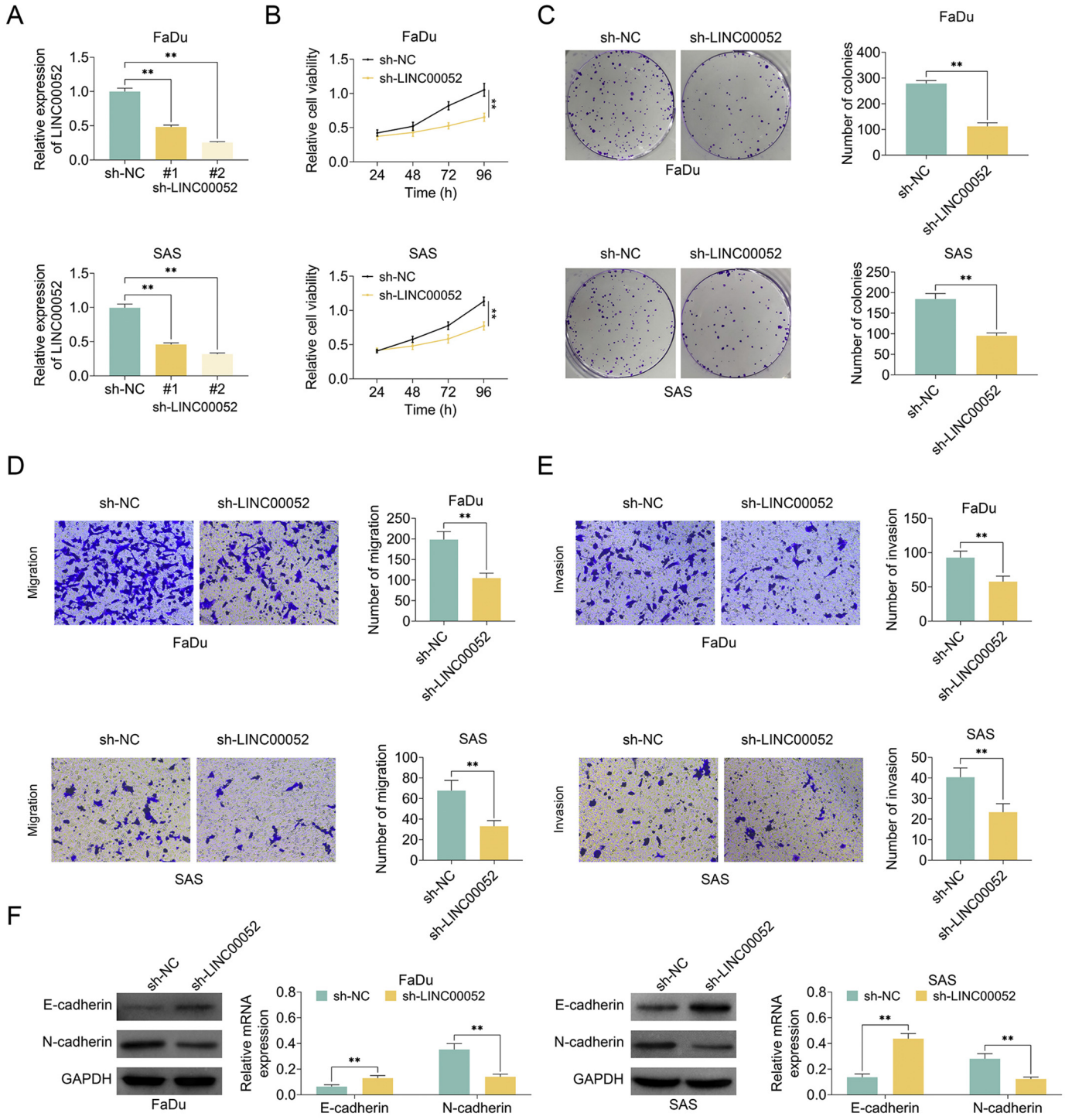

Fig. 3. Knockdown of LINC00052 inhibited HNSCC cell proliferation, migration and invasion.
(A) FaDu and SAS HNSCC cells were transfected with pLKO.1-sh-NC (shRNA not targeting any genes), pLKO.1-sh-LINC00052#1, or pLKO.1-sh-LINC00052#2. The RNA levels of LINC00052 were analysed via RT-qPCR assay. (B) FaDu and SAS HNSCC cells were transfected as in (A). Transfected cells were subjected to CCK-8 assay. (C–F) FaDu cells and SAS cells were transfected with pLKO.1-sh-NC or pLKO.1-sh-LINC00052 (sh-LINC00052#2). Transfected cells were subjected to colony formation assay (C), cell migration assay (D), cell invasion assay (E), and western blotting assay with the indicated antibodies (protein expression was normalized to GAPDH and shown as relative protein expression) (F). The data are presented as the mean ± SD of three independent experiments. Significant differences were calculated using student's t-test. $^{*}p < .05$, $^{**}p < .01$.

Next we examined whether LINC00052 regulates the level of miR-608. RT-qPCR data showed that expression of miR-608 was increased when LINC00052 were depleted, and reduced when LINC00052 were overexpressed in HNSCC cells (Fig. 4F). We also found that expression of miR-608 was significantly lower in HNSCC tumors than in adjacent nontumorous tissues (Fig. 4G). Expression of miR-608 was inversely correlated with expression of LINC00052 in HNSCC tumors (Fig. 4H).

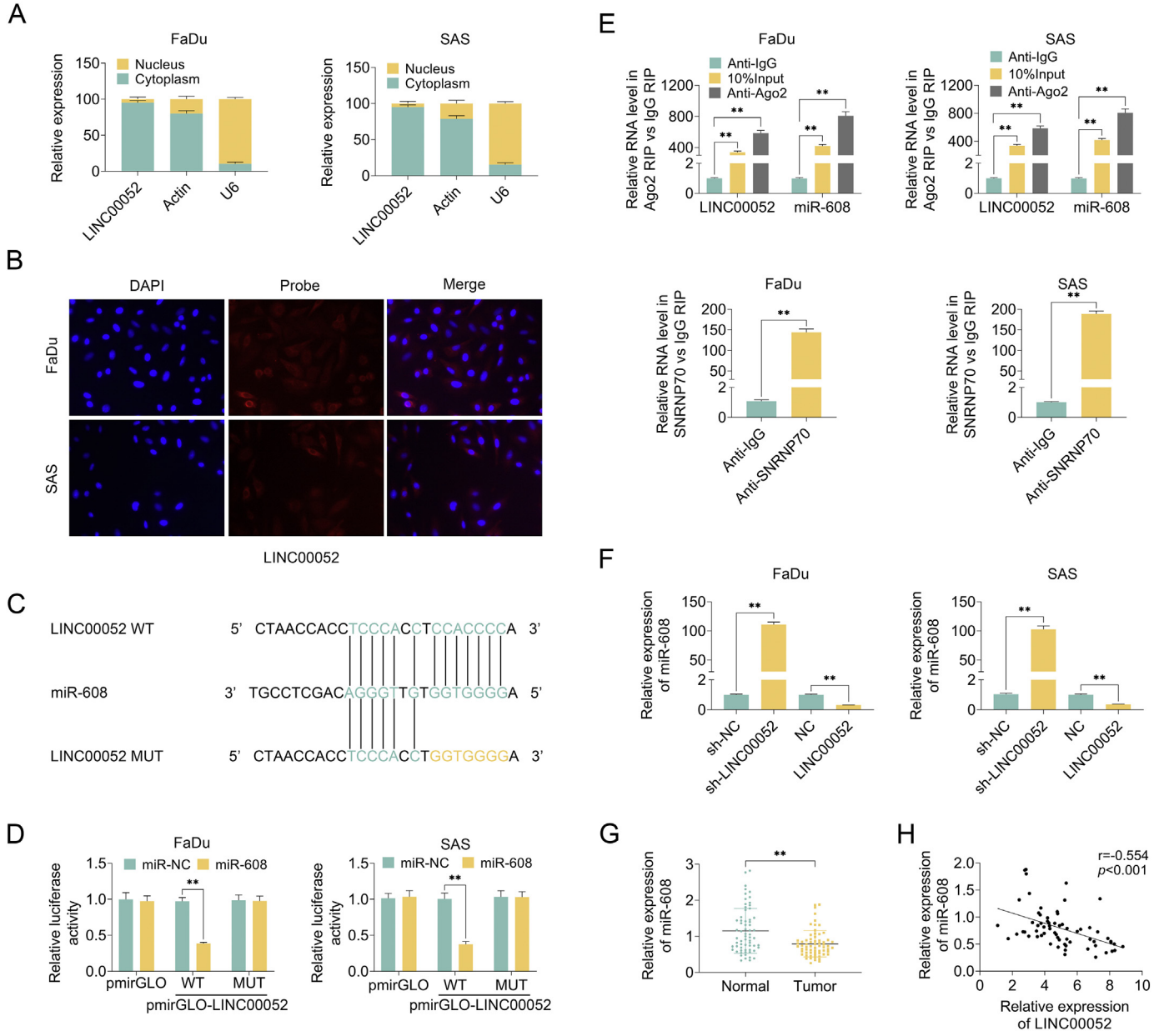

Fig. 4. LINC00052 interacted with and regulated miR-608 in HNSCC cells.
(A) FaDu cells and SAS cells were fractionated into nuclear and cytosol fractions. The RNAs of each fraction were extracted and subjected to RT-qPCR. (B) The distribution of LINC00052 was detected through FISH assay. DAPI was used to stain nuclei. (C) Predicted binding site of miR-608 within LINC00052 by microRNA target prediction tool miRSearch. The mutated binding site on LINC00052 was also shown. (D) FaDu cells and SAS cells were transfected with pmirGLO vector, wildtype (WT) or mutated (MUT) pmirGLO-LINC00052, together with miR-NC or miR-608 mimic. Dual luciferase assay was performed 48 h post-transfection. (E) FaDu and SAS cell lysates were immunoprecipitated with Ago2 antibody or control IgG. The immuno-precipitates were subjected to western blotting assay with Ago2 antibody (left), and RT-qPCR assay to monitor RNA levels of LINC00052 and miR-608 (right). (F) FaDu cells and SAS cells were transfected with pLKO.1-sh-NC, pLKO.1-sh-LINC00052, pcDNA3.1 vector (NC) or pcDNA3.1-LINC00052 plasmid. The expression levels of miR-608 were detected via RT-qPCR assay 48 h post-transfection. (G) Expression levels of miR-608 in tumor tissues or adjacent normal tissues obtained from 65 HNSCC patients were analysed via RT-qPCR assay. (H) Correlation between LINC00052 expression and miR-608 expression in HNSCCC tumors was determined by Spearman's correlation analysis. The data presented as the mean ± SD of three independent experiments. Significant differences were calculated using student's *t*-test (two groups) or one-way ANOVA (more than two groups). $*p < .05$, $**p < .01$.

3.4. miR-608 targeted EGFR mRNA in HNSCC cells

To further demonstrate how LINC00052 regulates HNSCC through miR-608, we take advantage of a miRNA target prediction tool miRDB (http://mirdb.org). EGFR was predicted to be a target gene of miR-608 using this online tool (Fig. 5A). Luciferase reporters were generated by cloning wildtype or mutated 3′ UTR of EGFR into vector pmirGLO (Fig. 5A). As shown in Fig. 5B, miR-608 mimic reduced the luciferase activity of wildtype pmirGLO-EGFR, but not the mutated pmirGLO-EGFR. To test whether miR-608 downregulated EGFR in HNSCC cells, miR-608 mimic and inhibitor were transfected into HNSCC cells respectively. RT-qPCR assays and western blotting assays revealed that miR-608 mimic reduced EGFR expression, while miR-608 inhibitor increased EGFR expression (Fig. 5C–E). In the paired samples from HNSCC patients, EGFR expression in HNSCC tumors was significantly higher than that in adjacent nontumorous tissues (Fig. 5F–G).

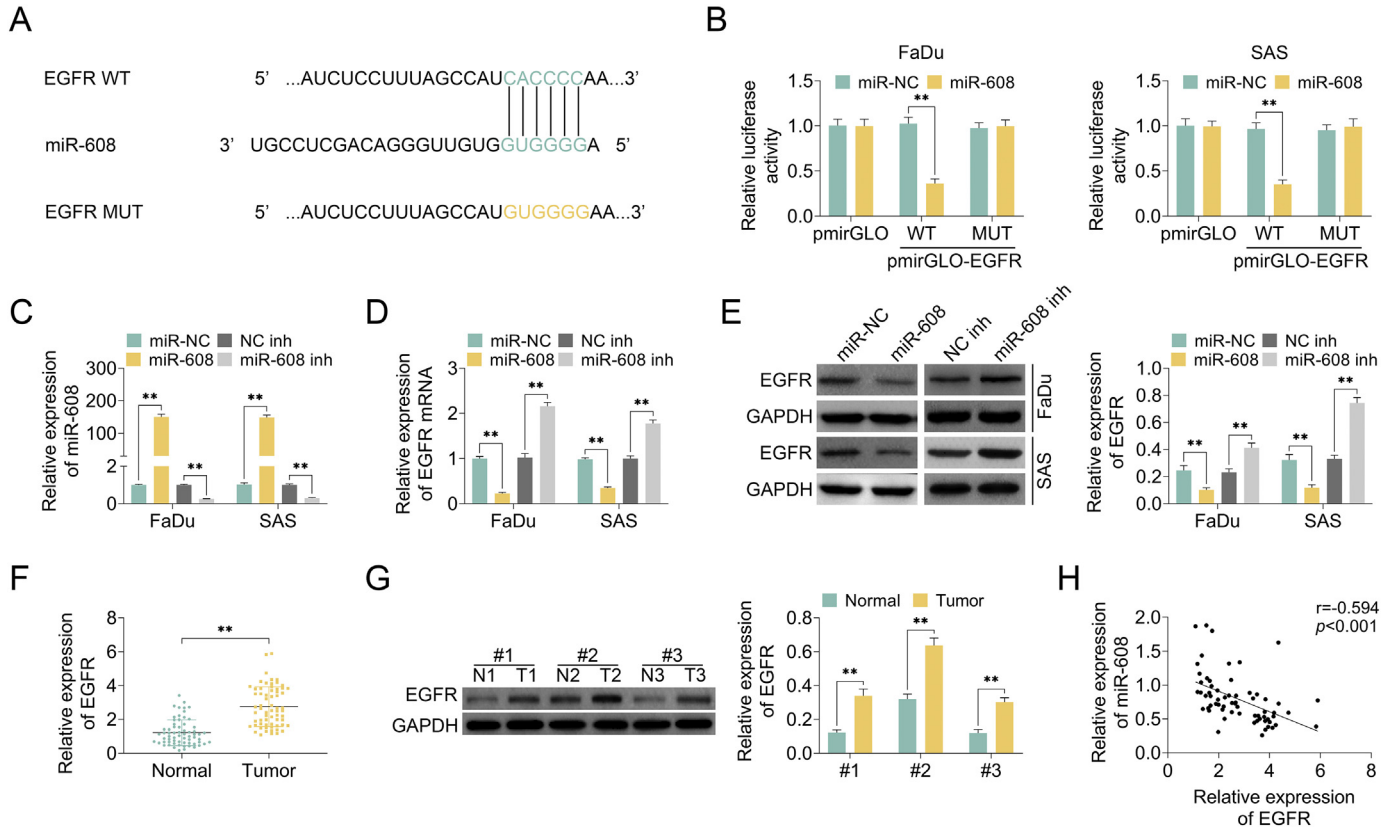

Fig. 5. MiR-608 targeted EGFR mRNA in HNSCC cells.
(A) Predicted binding site of miR-608 within EGFR mRNA by online software miRDB. The mutated binding site on EGFR mRNA was also shown. (B) FaDu cells and SAS cells were transfected with pmirGLO vector, wildtype (WT) or mutated (MUT) pmirGLO-EGFR, together with miR-NC or miR-608 mimic. Dual luciferase assay was performed 48 h post-transfection. (C-E) FaDu cells and SAS cells were transfected with miR-NC, miR-608 mimic, NC inhibitor or miR-608 inhibitor. The expression levels of miR-608 (C) and EGFR (D) was detected via RT-qPCR assay 48 h post-transfection. The expression levels of EGFR were also analysed via western blotting assay (protein expression was normalized to GAPDH and shown as relative protein expression) (E). (F) mRNA levels of EGFR in tumor tissues or adjacent normal tissues obtained from 65 HNSCC patients were analysed via RT-qPCR assay. (G) Western blotting assay was performed to monitor the protein expression levels of EGFR in 3 random pairs of patient tissues (protein expression was normalized to GAPDH and shown as relative protein expression). (H) Correlation between of EGFR mRNA expression and miR-608 expression in earlier referenced HNSCCC patient tissues was determined by Spearman's correlation analysis. The data presented as the mean ± SD of three independent experiments. Significant differences were calculated using student's *t*-test. $^{*}p < .05$, $^{**}p < .01$.

Expression of miR-608 was inversely correlated with mRNA expression of EGFR in HNSCC tumors (Fig. 5H).

3.5. LINC00052 regulated HNSCC cell proliferation, migration and invasion through modulating miR-608 and EGFR

Since miR-608 regulates EGFR expression and LINC00052 regulates miR-608, we hypothesized that LINC00052 could modulate EGFR expression and therefore proliferation, migration and invasion of HNSCC cells. Since SAS cells showed similar phenotype to FaDu cells, the further experiments were performed only on FaDu cells. We depleted LINC00052 in FaDu cells by shRNA. For the rescue experiment, we introduced miR-608 inhibitor or EGFR plasmid in the presence of LINC00052 shRNA (pcDNA3.1 vector showed similar phenotype with NC inhibitor (data not shown). NC inhibitor also served as the vector control of EGFR here). As expected, depletion of LINC00052 reduced EGFR expression, and miR-608 inhibitor abolished this reduction (Fig. 6A).

To investigate whether LINC00052 regulates HNSCC cell proliferation, migration and invasion through modulating miR-608 and EGFR, we transfected FaDu cells as in Fig. 6A, and then performed corresponding experiments. As shown in Fig. 3, depletion of LINC00052 decreased proliferation, migration, invasion and EMT potential of FaDu cells. However, miR-608 inhibitor and overexpression of EGFR abrogated the decrease (Fig. 6B–F). These data together demonstrated that LINC00052 regulated HNSCC cell proliferation, migration and invasion through regulating miR-608 and EGFR.

3.6. Depletion of LINC00052 suppressed HNSCC tumor growth in vivo

To determine the effect of LINC00052 on HNSCC in vivo, a xenograft tumor model was established in athymic nude mice using FaDu cells transfected with sh-NC, sh-LINC00052 or sh-LINC00052 plus miR-608 inhibitor. The tumors in the sh-LINC00052 group grew significantly slower than the ones in the sh-NC group, as shown by the tumor sizes, volumes and weights (Fig. 7A), which indicated that LINC00052 regulated HNSCC tumor growth in vivo. We also observed that the tumors with the miR-608 inhibitor and sh-LINC00052 grew faster than the tumors with only sh-LINC00052, and showed comparable tumor growth to the sh-NC group (Fig. 7A). These data indicated miR-608 inhibitor rescued the inhibition of HNSCC tumor growth caused by sh-LINC00052, demonstrating LINC00052 functioned through modulating miR-608 in vivo. Additionally, immunohistochemistry (IHC) analysis showed that the tumors from the sh-LINC00052 group displayed weaker Ki-67 and EGFR staining, and stronger E-cadherin than those from sh-NC group (Fig. 7B). Also, miR-608 inhibitor abrogated the effect of sh-LINC00052 (Fig. 7B). These results indicated LINC00052 regulated HNSCC progression in vivo.

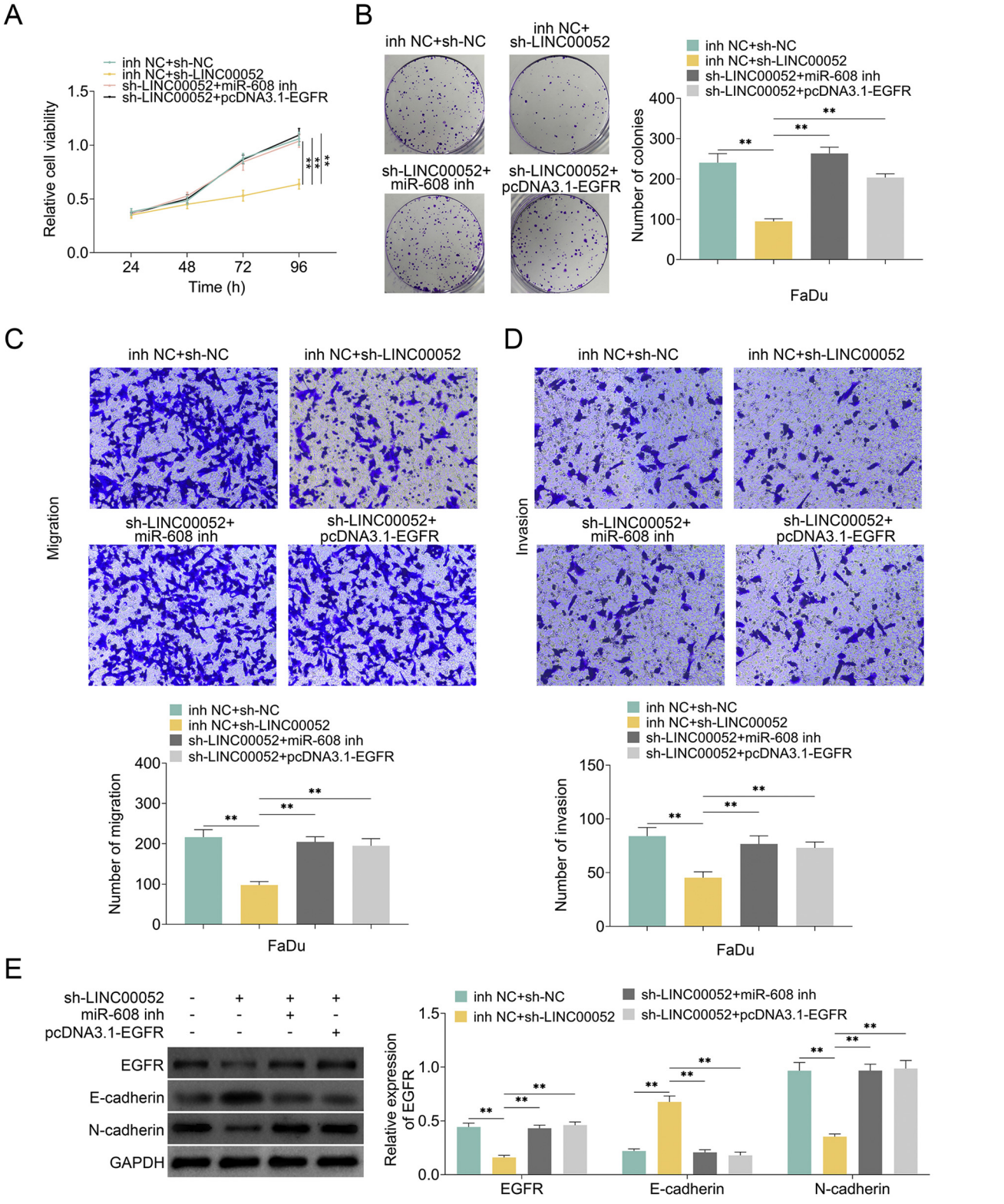

Fig. 6. LINC00052 promoted HNSCC cell proliferation, migration and invasion through regulating miR-608 and EGFR.
FaDu cells were transfected as follows: (Jou and Hess, 2017) NC inhibitor (inh NC) + NC shRNA (sh-NC), (Kolenda et al., 2017) NC inhibitor + sh-LINC00052, (Leemans et al., 2018) sh-LINC00052 + miR-608 inhibitor, (Wang et al., 2018) sh-LINC00052 + pcDNA3.1-EGFR. Transfected cells were subjected to RT-qPCR (A), CCK-8 assay (B), colony formation assay (C), cell migration assay (D), cell invasion assay (E), and western blotting assay with the indicated antibodies (protein expression was normalized to GAPDH and shown as relative protein expression) (F). The data presented as the mean ± SD of three independent experiments. Significant differences were calculated using one-way ANOVA. $^{*}p < .05$, $^{**}p < .01$.

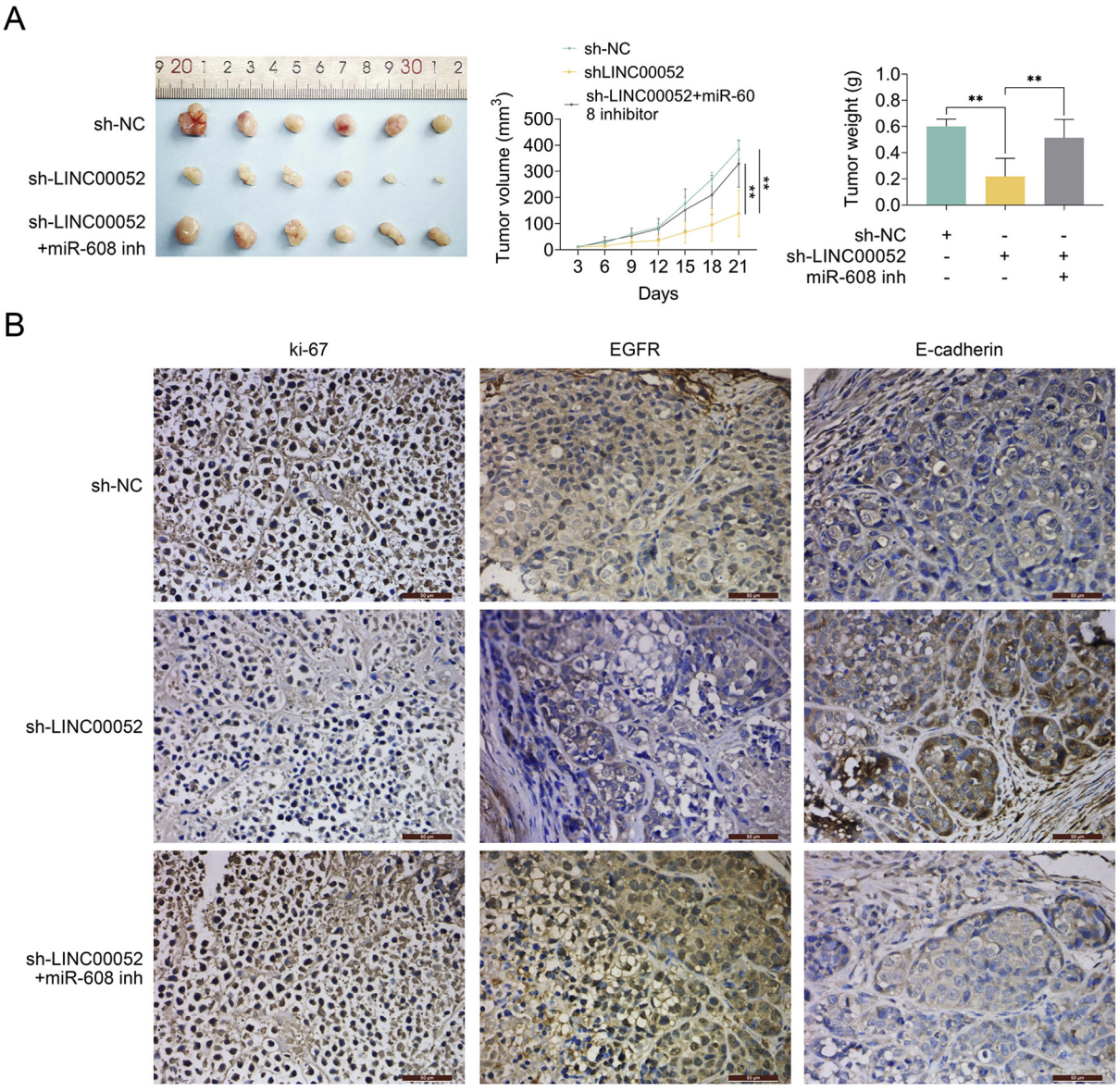

Fig. 7. Knockdown of LINC00052 suppressed HNSCC tumor growth in vivo. FaDu cells were transfected with NC shRNA, shLINC00052, or shLINC00052 plus miR-608 inhibitor. The transfected cells were inoculated into nude mice. When tumors were first palpable, the mice were intratumorally injected with Lipofectamine 3000-encapsulated sh-NC, sh-LINC00052, or sh-LINC00052 plus miR-608 inhibitor every 3 days respectively. (A) The tumor volume was calculated every 3 days (middle). 21 days post-inoculation, mice were sacrificed and the tumors were removed (left) and weighted (right). (B) IHC assay was performed to detect the expression of ki-67, EGFR and E-cadherin in FaDu tumors. Significant differences were calculated using one-way ANOVA. $*p < .05$, $**p < .01$.

4. Discussion

An increasing number of studies have shown that lncRNAs were involved in carcinogenesis (Diamantopoulos et al., 2018; Liz and Esteller, 2016). LINC00052 is a newly identified lncRNA associated with cancer development. LINC00052 activated HER3 signalling (Salameh et al., 2017) and Wnt/β-Catenin signalling (Shan et al., 2017) to promote cancer progression in breast cancer and gastric cancer, respectively. However, in hepatocellular carcinoma (Xiong et al., 2016; Zhu et al., 2017), pancreatic cancer (Xiong et al., 2019), and colorectal cancer (Yu et al., 2019), LINC00052 was shown to inhibit cancer procession and function as a tumor suppressor. Data from this study revealed that LINC00052 promoted HNSCC progression. LINC00052 was upregulated in HNSCC tumors and cells (Fig. 1). High expression of LINC00052 was associated with worse prognosis (Fig. 1C, Tables 1–2). Data from gain and loss of function experiments revealed that LINC00052 promoted HNSCC cell proliferation, migration and invasion (Figs. 2–3).

Competing endogenous RNA (ceRNA) network is a new regulatory network discovered a decade ago (Ebert et al., 2007; Franco-Zorrilla et al., 2007; Seitz, 2009; Poliseno et al., 2010). In this network, RNA transcripts compete for miRNA binding, thereby alleviating the effect of miRNA on their mRNA target (Salmena et al., 2011). These RNA transcripts are known as ceRNAs, or microRNA sponges/decoys (Salmena et al., 2011). Many lncRNAs have been reported to function as ceRNAs to sequester miRNAs from their target mRNAs (Liz and Esteller, 2016), which remind us LINC00052 may also act as a ceRNA. Cytoplasmic and nuclear fractionation and FISH assay revealed that LINC00052 was mainly distributed in cytoplasm (Fig. 4A–B), which supported the ceRNA hypothesis. Through bioinformatics analysis and subsequent confirming assays, we demonstrated LINC00052 interacted with miR-608 (Fig. 4) and miR-608 targeted the mRNA of EGFR (Fig. 5). In addition, data from in vitro (Fig. 6) and in vivo (Fig. 7) assays revealed that LINC00052 acted as a ceRNA for miR-608, thereby

regulating the level of EGFR and promoting HNSCC progression.

MiR-608 was found to be downregulated in various cancers and act as a tumor suppressor (Liang et al., 2017). MiR-608 inhibits proliferation of bladder cancer via directly targeting FLOT1, and suppressing the downstream AKT/FOXO3a signalling (Liang et al., 2017). AKT2 was targeted by miR-608 in lung adenocarcinoma, which promoted the apoptosis of cancer cells (Othman and Nagoor, 2017). MiR-608 also targeted macrophage migration inhibitory factor (MIF) in glioma stem cells (Wang et al., 2016a), hepatocellular carcinoma (Wang et al., 2016b) and lung adenocarcinoma (Yu et al., 2018) to suppress cancer cell migration and invasion. N-a-acetyltransferase NAA10 was targeted and downregulated by miR-608 in colon cancer, resulting in suppression of cell proliferation and migration and promoted apoptosis (Yang et al., 2016). Oncogenes EGFR and Bcl-xL were also identified as targets of miR-608 in chordoma cells (Zhang et al., 2014). MiR-608 inversely correlated with EGFR expression in chordoma cells, and inhibited cancer cell proliferation, survival and invasion (Zhang et al., 2014). In the current study, we also identified EGFR as a target of miR-608 in HNSCC (Fig. 5A–E). In addition, our data showed that miR-608 inversely correlated with EGFR expression in tumor tissue samples obtain from HNSCC patients (Fig. 5H). Therefore, our study supports a tumor suppressor role of miR-608, which functions by targeting EGFR in HNSCC cells.

In conclusion, data from this study revealed that LINC00052 was upregulated in HNSCCs and higher expression correlated with poor prognosis. LINC00052 sponged miR-608, thereby alleviating the silencing effect of miR-608 on EGFR, and promoting HNSCC proliferation, migration and invasion. Findings of our study indicate LINC00052 is an oncogene in HNSCCs and suggest LINC00052 is a potential therapeutic target for HNSCCs.

Funding

This work was supported by Medical Health Science and Technology Project of Zhejiang Provincial Health Commission (Grant No. 2019314890).

Availability of data and materials

All data generated or analysed during this study are included in this published article.

Authors' contributions

TBOY and YZ conceived and designed the experiments , SXT analysed and interpreted the results of the experiments, YWW performed the experiments.

Ethics approval and consent to participate

The animal use protocol listed below has been reviewed and approved by the Animal Ethical and Welfare Committee.

Patient consent for publication

Not Applicable.

Informed consent

Written informed consent was obtained from a legally authorized representative(s) for anonymized patient information to be published in this article.

Declaration of Competing Interest

The authors declare that they have no competing interests, and all authors should confirm its accuracy.

Acknowledgements

Not applicable.

References

Bartel, D.P., 2009. MicroRNAs: target recognition and regulatory functions. Cell. 136 (2), 215–233.
Bartel, D.P., 2018. Metazoan MicroRNAs. Cell. 173 (1), 20–51.
Bei, R., Budillon, A., Masuelli, L., Cereda, V., Vitolo, D., Di Gennaro, E., et al., 2004. Frequent overexpression of multiple ErbB receptors by head and neck squamous cell carcinoma contrasts with rare antibody immunity in patients. J. Pathol. 204 (3), 317–325.
Diamantopoulos, M.A., Tsiakanikas, P., Scorilas, A., 2018. Non-coding RNAs: the riddle of the transcriptome and their perspectives in cancer. Ann. Transl. Med. 6 (12), 241.
Ebert, M.S., Neilson, J.R., Sharp, P.A., 2007. MicroRNA sponges: competitive inhibitors of small RNAs in mammalian cells. Nat. Methods 4 (9), 721–726.
Fabian, M.R., Sonenberg, N., Filipowicz, W., 2010. Regulation of mRNA translation and stability by microRNAs. Annu. Rev. Biochem. 79, 351–379.
Franco-Zorrilla, J.M., Valli, A., Todesco, M., Mateos, I., Puga, M.I., Rubio-Somoza, I., et al., 2007. Target mimicry provides a new mechanism for regulation of microRNA activity. Nat. Genet. 39 (8), 1033–1037.
Fung, C., Zhou, P., Joyce, S., Trent, K., Yuan, J.M., Grandis, J.R., et al., 2015. Identification of epidermal growth factor receptor (EGFR) genetic variants that modify risk for head and neck squamous cell carcinoma. Cancer Lett. 357 (2), 549–556.
Guglas, K., Bogaczynska, M., Kolenda, T., Rys, M., Teresiak, A., Blizniak, R., et al., 2017. lncRNA in HNSCC: challenges and potential. Contemp. Oncol. 21 (4), 259–266.
Jou, A., Hess, J., 2017. Epidemiology and molecular biology of head and neck Cancer. Oncol. Res. Treat. 40 (6), 328–332.
Kolenda, T., Guglas, K., Rys, M., Bogaczynska, M., Teresiak, A., Blizniak, R., et al., 2017. Biological role of long non-coding RNA in head and neck cancers. J. Greatpoland Cancer Center Poznan Polish Soc. Radiat. Oncol. 22 (5), 378–388.
Leemans, C.R., Snijders, P.J.F., Brakenhoff, R.H., 2018. The molecular landscape of head and neck cancer. Nat. Rev. Cancer 18 (5), 269–282.
Liang, Z., Wang, X., Xu, X., Xie, B., Ji, A., Meng, S., et al., 2017. MicroRNA-608 inhibits proliferation of bladder cancer via AKT/FOXO3a signaling pathway. Mol. Cancer 16 (1), 96.
Liz, J., Esteller, M., 2016. lncRNAs and microRNAs with a role in cancer development. Biochim. Biophys. Acta 1859 (1), 169–176.
Ni, X., Liao, Y., Li, L., Zhang, X., Wu, Z., 2018. Therapeutic role of long non-coding RNA TCONS_00019174 in depressive disorders is dependent on Wnt/beta-catenin signaling pathway. J. Integr. Neurosci. 17 (2), 125–132.
Oda, K., Matsuoka, Y., Funahashi, A., Kitano, H., 2005. A comprehensive pathway map of epidermal growth factor receptor signaling. Mol. Syst. Biol. 2005 (0010), 1.
Ongkeko, W.M., Altuna, X., Weisman, R.A., Wang-Rodriguez, J., 2005. Expression of protein tyrosine kinases in head and neck squamous cell carcinomas. Am. J. Clin. Pathol. 124 (1), 71–76.
Othman, N., Nagoor, N.H., 2017. miR-608 regulates apoptosis in human lung adenocarcinoma via regulation of AKT2. Int. J. Oncol. 51 (6), 1757–1764.
Poliseno, L., Salmena, L., Zhang, J., Carver, B., Haveman, W.J., Pandolfi, P.P., 2010. A coding-independent function of gene and pseudogene mRNAs regulates tumour biology. Nature. 465 (7301), 1033–1038.
Salameh, A., Fan, X., Choi, B.K., Zhang, S., Zhang, N., An, Z., 2017. HER3 and LINC00052 interplay promotes tumor growth in breast cancer. Oncotarget. 8 (4), 6526–6539.
Salmena, L., Poliseno, L., Tay, Y., Kats, L., Pandolfi, P.P., 2011. A ceRNA hypothesis: the Rosetta stone of a hidden RNA language? Cell. 146 (3), 353–358.
Seitz, H., 2009. Redefining microRNA targets. Current Biol: CB. 19 (10), 870–873.
Shan, Y., Ying, R., Jia, Z., Kong, W., Wu, Y., Zheng, S., et al., 2017. LINC00052 promotes gastric Cancer cell proliferation and metastasis via activating the Wnt/beta-catenin Signaling pathway. Oncol. Res. 25 (9), 1589–1599.
Wang, Z., Xue, Y., Wang, P., Zhu, J., Ma, J., 2016a. MiR-608 inhibits the migration and invasion of glioma stem cells by targeting macrophage migration inhibitory factor. Oncol. Rep. 35 (5), 2733–2742.
Wang, K., Liang, Q., Wei, L., Zhang, W., Zhu, P., 2016b. MicroRNA-608 acts as a prognostic marker and inhibits the cell proliferation in hepatocellular carcinoma by macrophage migration inhibitory factor. J. Int. Soc. Oncodevelopmental Biol. Med. 37 (3), 3823–3830.
Wang, R., Ma, Z., Feng, L., Yang, Y., Tan, C., Shi, Q., et al., 2018. LncRNA MIR31HG targets HIF1A and P21 to facilitate head and neck cancer cell proliferation and tumorigenesis by promoting cell-cycle progression. Mol. Cancer 17 (1), 162.
Xiong, D., Sheng, Y., Ding, S., Chen, J., Tan, X., Zeng, T., et al., 2016. LINC00052 regulates the expression of NTRK3 by miR-128 and miR-485-3p to strengthen HCC cells invasion and migration. Oncotarget. 7 (30), 47593–47608.
Xiong, X., Shi, Q., Yang, X., Wang, W., Tao, J., 2019. LINC00052 functions as a tumor suppressor through negatively modulating miR-330-3p in pancreatic cancer. J. Cell. Physiol. 234 (9), 15619–15626.
Yang, H., Li, Q., Niu, J., Li, B., Jiang, D., Wan, Z., et al., 2016. microRNA-342-5p and miR-608 inhibit colon cancer tumorigenesis by targeting NAA10. Oncotarget. 7 (3), 2709–2720.
Yu, H.X., Wang, X.M., Han, X.D., Cao, B.F., 2018. MiR-608 exerts tumor suppressive

function in lung adenocarcinoma by directly targeting MIF. Eur. Rev. Med. Pharmacol. Sci. 22 (15), 4908–4916.
Yu, G., Xiong, D., Liu, Z., Li, Y., Chen, K., Tang, H., 2019. Long noncoding RNA LINC00052 inhibits colorectal cancer metastasis by sponging microRNA-574-5p to modulate CALCOCO1 expression. J. Cell. Biochem. 120 (10), 17258–17272.
Zhang, H., Berezov, A., Wang, Q., Zhang, G., Drebin, J., Murali, R., et al., 2007. ErbB receptors: from oncogenes to targeted cancer therapies. J. Clin. Invest. 117 (8), 2051–2058.
Zhang, Y., Schiff, D., Park, D., Abounader, R., 2014. MicroRNA-608 and microRNA-34a regulate chordoma malignancy by targeting EGFR, Bcl-xL and MET. PLoS One 9 (3), e91546.
Zhu, L., Yang, N., Chen, J., Zeng, T., Yan, S., Liu, Y., et al., 2017. LINC00052 upregulates EPB41L3 to inhibit migration and invasion of hepatocellular carcinoma by binding miR-452-5p. Oncotarget. 8 (38), 63724–63737.